Original Article

Detection and Evaluation of Intracranial Aneurysms in the Posterior Fossa by Multidetector Computed Tomography Angiography – Comparison with Digital Subtraction Angiography

Vivek Singh, S. Vignesh, Zafar Neyaz, Rajendra Vishnu Phadke, Anant Mehrotra[1], Prabhakar Mishra[2]

Departments of Radiodiagnosis, [1]Neurosurgery and [2]Biostatistics, SGPGIMS, Lucknow, Uttar Pradesh, India

Abstract

Introduction: Posterior fossa hemorrhages are not so frequent but as posterior cranial fossa space is narrow and has many vital structures, even a small amount of bleed can lead to compression of brain stem and serious consequences. Identification and planning management of cause of bleed requires angiogram. Digital subtraction angiography (DSA) being invasive modality but is gold standard, so noninvasive computed tomography angiography (CTA) is compared to detect cause of bleed in the posterior fossa in this study. **Materials and Methods:** From January 2017 to October 2018, all patients with posterior fossa bleed who underwent CTA and DSA for evaluation were compared regarding identification of aneurysm as cause of bleed. **Results:** A total of 49 patients were evaluated in this study during study duration, of which 26 (53%) were male and 23 (47%) were female. Out of 49 patients evaluated, 47 patients had aneurysms detected on DSA. Of 25 patients who underwent both procedures, 23 patients had aneurysms, and correct diagnosis was made with CTA in 24 out of 25 aneurysms. One aneurysm missed by CTA was close to bony structure. **Discussion:** With advancement of CTA technology, sensitivity of detecting intracranial aneurysms has increased to >96%. The overall sensitivity in detecting aneurysms is 96% with sensitivity in detecting aneurysms >4 mm being 100%. The sensitivity of CTA for smaller sized aneurysms is low which is attributed partially to lower spatial resolution of CT compared to DSA. **Conclusion:** CTA is a simple, fast, and noninvasive imaging modality that can be used to detect and characterize intracranial aneurysms in the posterior fossa.

Keywords: *Computed tomography angiography, digital subtraction angiography, posterior fossa aneurysms, posterior fossa bleed*

Introduction

Intracranial aneurysmal rupture is the most common cause of nontraumatic subarachnoid hemorrhage (SAH)[1-5] overall and also in the posterior fossa. Posterior fossa hemorrhages are not so frequent as compared to lesions in the anterior and middle cranial fossa. However, due to the narrow space of the posterior cranial fossa and the presence of many vital structures, even a small amount of bleed can lead to compression of brain stem and serious consequences. Immediate surgical treatment is needed for posterior fossa bleeds as compared to supratentorial bleeds.[6,7] To prevent mortality and morbidity, rapid diagnosis of the bleed and the underlying cause is of utmost importance.

Digital subtraction angiography (DSA) is a gold standard for diagnosis and characterization of intracranial aneurysms.[2,5,8] DSA has some advantages such as large field of view, high spatial resolution, and temporal imaging capabilities, yet it is invasive, time-consuming, and operator-dependent technique. The overall incidence of procedure-related neurological complications in DSA is around 1%–2.6%[9] and that of persistent neurological deficits is around 0.1%–0.5%.[6,10,11] With recent advancements, multidetector computed tomography angiography (MDCTA) has gained in importance on par with DSA, for detection of intracranial aneurysms. CTA is easy to perform and noninvasive and can be done immediately after confirmation of SAH. The lack of periprocedural neurological complications, which are associated with DSA, adds to advantage for CTA. However, CTA has

Address for correspondence: *Dr. Vivek Singh, Department of Radiodiagnosis, SGPGIMS, Lucknow, Uttar Pradesh, India. E-mail: singhvivek79@rediffmail.com*

Access this article online

Website: www.asianjns.org

DOI: 10.4103/ajns.AJNS_290_18

Quick Response Code:

How to cite this article: Singh V, Vignesh S, Neyaz Z, Phadke RV, Mehrotra A, Mishra P. Detection and evaluation of intracranial aneurysms in the posterior fossa by multidetector computed tomography angiography – Comparison with digital subtraction angiography. Asian J Neurosurg 2019;14:491-8.

not been able to replace DSA completely for detection of intracranial aneurysms. This is thought to be due to lower spatial resolution of CTA compared to DSA and the technical parameters which are very important for CTA. Concentration and dose of contrast agent, injection rate, weight of the patient, hemodynamic factors, and proper timing of the scan affect the quality of the imaging.

Even though there were many studies done previously to compare the diagnostic efficacy of CTA and DSA in SAH and in the detection and evaluation of intracranial aneurysms, none of these studies were specific for comparing the diagnostic efficacy in the posterior fossa. Therefore, the present study aims to compare CTA with DSA in detection of intracranial aneurysms limited to the posterior fossa.

Materials and Methods

Patients

Our study group consisted of 49 patients from January 2017 to October 2018 who were admitted in our hospital (Sanjay Gandhi Postgraduate Institute of Medical Sciences, Lucknow, Uttar Pradesh, India) with symptoms of posterior fossa SAH. Twenty-six (53%) patients were male and 23 (47%) were female. The mean age of the patients was 47.4 ± 1.8 years (range: 20–75 years). The diagnosis of SAH was established by noncontrast CT scan. Patients with posterior fossa SAH as a part of supratentorial pathology were excluded from the study. Among 49 patients who were admitted with SAH, 25 patients underwent both CTA and DSA, with a mean interval time of 4.3 ± 0.8 days (range: 0–14 days). Rest of the 24 patients underwent only DSA.

Imaging protocol

Computed tomography angiography

CT angiography was performed on a 64-detector MDCT system (Brilliance; Philips medical systems, New Virginia, USA). The area covered was from C2 vertebra to the top of cranial vault, with the patient positioned supine and head immobilization achieved using adhesive strap. Nonionic contrast medium (80–100 ml) was injected at a rate of 5 ml/s followed by saline flush of 40 ml through a cannula in the upper limb vein or central line, using Medrad Stellant pressure injector. CT parameters were as follows: 0.75 s/r gantry rotation speed, 512 × 512 matrix, 0.6–0.9 pitch, 64 × 0.625 slice collimation, 220–240-mm field of view, 120-kVp tube voltage, and 400-mA tube current. Data acquisition was started by monitoring contrast arrival in arteries using smart prep (bolus tracking method). The scan was started manually once the contrast reached the common carotid artery. The source images were transferred to dedicated workstation – Extended Brilliance Workspace (Koninklijke Philips Electronics, Netherlands) for postprocessing and image review. Apart from the source images, the other methods utilized for better visualization included the multiplanar reformation (MPR), maximum intensity projection (MIP), and three-dimensional (3D) volume-rendering technique (VRT). 2D thin (3–4 mm) and thick slab MIP and MPR were used in all cases. 2D images were simultaneously analyzed in all the three planes – axial, sagittal, and coronal. 3D VRT was also used in almost all the cases.

Digital subtraction angiography

DSA was carried out on a Siemens Artis Zee Biplane or Philips Allura FD20 system by two experienced interventional radiologists. Selective four-vessel or six-vessel DSA through femoral artery catheterization was performed. Anteroposterior, lateral, oblique, and wherever necessary additional views of each vessel were obtained by manual injection of nonionic contrast media. The images obtained were then reviewed in the dedicated workstations.

Image analysis

Two experienced radiologists who had >10 years' experience in the field of interventional and neuroradiology analyzed the imaging independently; each being blinded to the other's readings and, in particular, blinded to the findings obtained by the other modality. The main vessels evaluated were the V4 segment of the vertebral artery (V4-VA), posterior inferior cerebellar arteries (PICAs), anterior inferior cerebellar arteries (AICAs), basilar artery (BA), and superior cerebellar arteries. The detected aneurysms were characterized based on its location, size and type, calcification, and intraluminal thrombi. All the aneurysms were assessed initially in source images, followed by MPR, MIP, and VRT images.

Statistical analysis

DSA was considered as the gold standard for the imaging of the intracranial aneurysms. The sensitivity, specificity, and diagnostic accuracy of the CTA in detection of posterior fossa aneurysms were compared with DSA. The sensitivity and specificity were calculated separately for the size of the aneurysms (<4, 4–7, 7–10, and >10mm). The comparison between the sizes of the aneurysms in two groups was made using paired *t*-test. The agreement between the two groups was made using the appropriate nonparametric tests of significance. $P < 0.05$ was considered to be statistically significant. The Statistical Package for the Social Sciences version 21 (SPSS-21, IBM, Chicago, Illinois, USA) was used for statistical analysis.

Results

A total of 49 patients were evaluated in this study during the study duration, of which 26 (53%) were male and 23 (47%) were female. The main presenting complaints being headache followed with vomiting, noted in 80% cases. The other complaints were transient loss of consciousness, seizures, vertigo, and neck pain. Hemorrhage at presentation was present in 95% of the cases. The hemorrhage was SAH with intraventricular hemorrhage (IVH) in 24 patients (49%), SAH without IVH in 12 (25%), and intraparenchymal hemorrhage in 6 patients (12%). Isolated IVH at presentation was noted in 2 patients (4%). The predominant noncontrast CT finding in patients not having hemorrhage was circular hyperdensity noted in 5 patients (10%). Hydrocephalus was noted in 16.3% cases (8 patients). In cases of SAH, according to the modified Fisher's grading, Grade IV (thick SAH + IVH) was noted in 47%, Grade III in 26%, Grade II in 16%, and Grade I in 11%.

Out of 49 patients evaluated, 47 patients had aneurysms, and no cause for SAH could be detected in 2 patients. Among 47 patients who had aneurysms, 24 (51.1%) were male and 23 (48.9%) were female. The age group ranged from 20 to 75 years with a mean age of 46.96 ± 1.88 years [Figure 1].

DSA detected 51 aneurysms in 47 patients. About 43 patients had one aneurysm and 4 patients had two aneurysms. The distribution of the aneurysms is given in Tables 1 and 2. The most common location of aneurysms was V4-VA (19 cases, 37.2%) followed by PICAs (13 cases, 25.5%). Out of 51 aneurysms, 23 (45.1%) were fusiform, 22 (43.1%) were saccular, 4 (7.8%) were associated with dissection, and 2 (3.9%) were pseudoaneurysms. Figure 2 shows dissecting V4 segment aneurysm – Figure 2a shows MIP CTA image, Figure 2b shows same in volume rendering, and Figure 2c shows same on DSA; Figure 3 shows PICA saccular aneurysm; Figure 4 shows AICA saccular aneurysm; Figure 5 shows AICA fusiform aneurysm; and Figure 6 shows vertebrobasilar artery aneurysm.

Accuracy of computed tomography angiography versus digital subtraction angiography

Out of the total of 49 patients evaluated, 25 patients underwent both the procedures (CTA and DSA). The patients who underwent both the procedures did not have any postprocedural contrast-related or catheter-related complications. Of the 25 patients who underwent both the procedures, 23 patients had aneurysms, and two patients had intraparenchymal hemorrhage which was negative on both CTA and DSA. The interval between the two procedures in patients having aneurysms was 4.3 ± 0.8 (0–14 days).

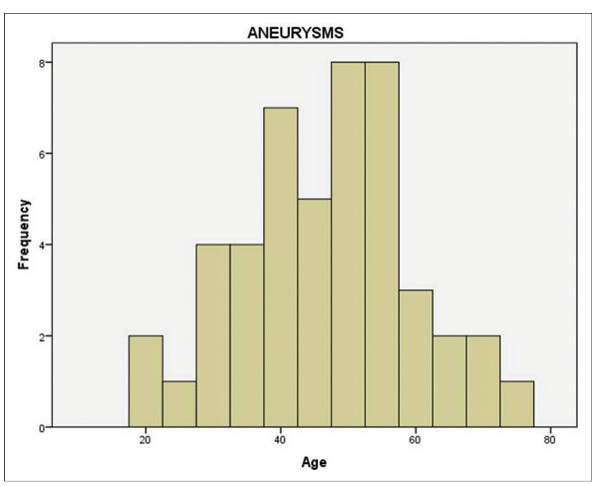

Figure 1: Age distribution among patients having aneurysms

Correct diagnosis was made with CTA in 24 out of 25 aneurysms. Two patients who had intraparenchymal hemorrhage were negative on CTA. There was excellent intermodality agreement (kappa value, $\kappa = 0.95$; $P < 0.05$) between CTA and DSA in localizing the aneurysm [Table 3]. On DSA, the size of the aneurysmal sac ranged from 2.7 to 25 mm with a mean size of 9.34 ± 1.13 mm. The mean size of the aneurysmal sac detected by CTA was 9.75 ± 1.3 mm with range of 3.2–27 mm. The smallest detectable sac size on CT was 3.2 mm. Out of the 24 aneurysms, 5 (20.8%) were <4 mm, 4 (16.7%) aneurysms between 4–7 mm, 9 (37.5%) aneurysms between 7–10 mm, and 6 (25%) aneurysms were >10 mm. There was no statistically significant difference between the sizes of the aneurysms between CTA and DSA ($P > 0.05$, paired *t*-test).

One aneurysm missed by CTA was of size range <4 mm and was located in distal right AICA, which was in proximity to the bony structures. However, subsequent analysis of the CT data set showed that aneurysm was visible on CTA

Table 1: Distribution of aneurysms according to their location

Location	*n* (%)
Vertebral artery - V4 segment	
Right	10 (19.6)
Left	9 (17.6)
Total	19 (37.2)
PICA	
Right	6 (11.8)
Left	7 (13.7)
Total	13 (25.5)
Anterior inferior cerebellar artery	
Right	2 (3.9)
Left	2 (3.9)
Total	4 (7.8)
Superior cerebellar artery	
Right	3 (5.9)
Left	1 (2.0)
Total	4 (7.8)
Vertebrobasilar junction	4 (7.8)
Mid BA	5 (9.8)
Vertebral artery - V3 segment	2 (3.9)

BA – Basilar artery; PICA – Posterior inferior cerebellar artery

Table 2: Distribution of aneurysms according to size

Size of aneurysm (mm)	*n* (%)
<4	8 (16)
4-7	13 (26)
7-10	12 (24)
>10	17 (34)

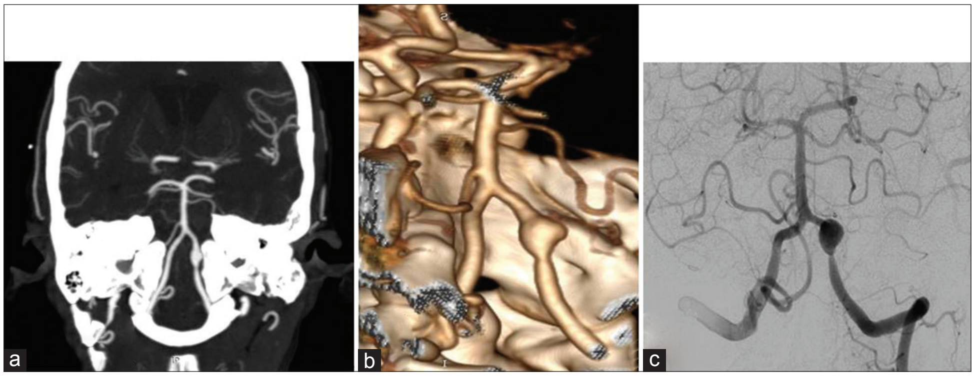

Figure 2: Left vertebral artery aneurysm. (a) Coronal maximum intensity projection image, (b) volume-reconstructed image, (c) digital subtraction angiography image in anteroposterior view of the same patient showing a fusiform dissecting aneurysm in the distal part of the V4 segment of the left vertebral artery

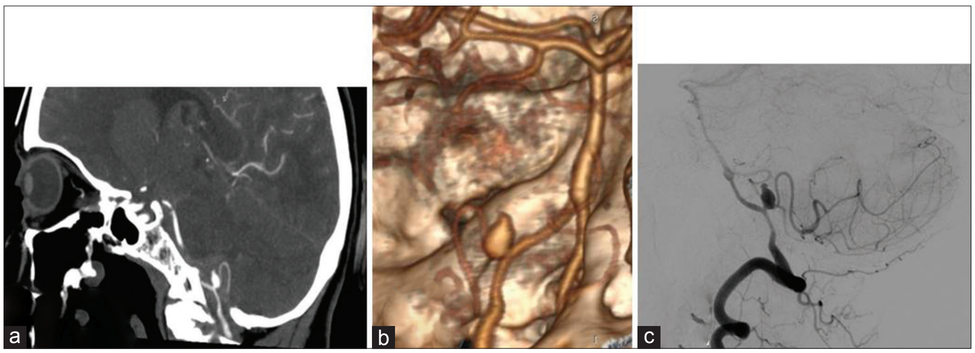

Figure 3: Right posterior inferior cerebellar artery aneurysm. (a) Sagittal maximum intensity projection image, (b) volume-reconstructed image, (c) digital subtraction angiography image in lateral view of the same patient showing a saccular aneurysm in the proximal part of posterior inferior cerebellar artery just after its origin. A nipple-like projection can be seen from its superior aspect in both computed tomography angiography and digital subtraction angiography images

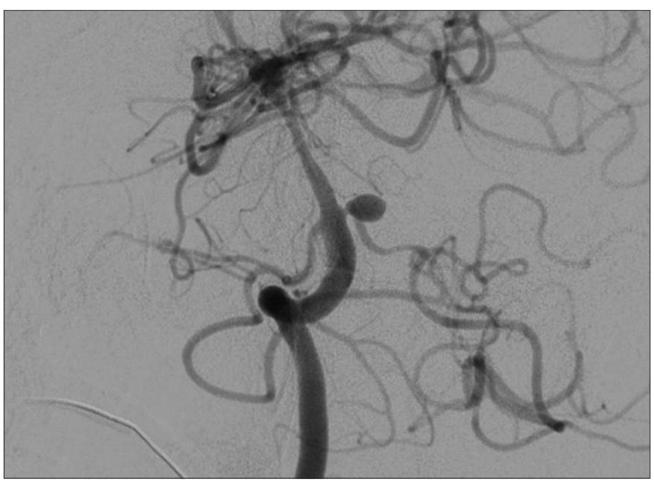

Figure 4: Digital subtraction angiography image in anteroposterior view showing saccular aneurysm arising from the left anterior inferior cerebellar artery

images (with MPR reconstruction and in MIP images) but was missed initially due to its size and its location adjacent to the bone. One aneurysm localized to the V4 segment of the right vertebral artery near the origin of the right PICA was actually located in the right PICA [Figure 3].

The sensitivity and specificity of CTA were calculated depending on the aneurysm size. The sensitivity of CTA in detecting aneurysms <4 mm was 83.3% compared to sensitivity of 100% in aneurysms >4 mm. The specificity was 100% for <4 mm and >4 mm [Table 4]. The positive predictive and negative predictive value for detecting aneurysms <4 mm was 100% and 95%, respectively. On per-patient basis, the sensitivity of CTA in detecting aneurysms as the cause of the hemorrhage was 95.7%. The diagnostic accuracy in terms of per-aneurysm basis and per-patient basis is given in Table 5. There was good measure of agreement between CTA and DSA in detecting the cause ($\kappa = 0.76 \pm 0.13$; $P < 0.05$).

In addition, CTA showed the presence of mural calcifications in the wall of four aneurysms. Intraluminal thrombus was detected in three aneurysms [Figures 7 and 8]. The presence of calcifications and thrombus could not be picked up by the DSA.

In three cases of aneurysms in V4 segments (right – 1, left – 2), the corresponding PICAs were incorporated within aneurysm, i.e., arising from the aneurysmal sac.

Out of 47 aneurysms detected, 27 underwent therapeutic procedures [Table 6]. Endovascular treatment was done in 26 patients, and operative clipping of aneurysm was done in only one patient. Among endovascular treatment, embolization of the aneurysms using endovascular coils

Figure 5: Digital subtraction angiography image in anteroposterior view showing fusiform aneurysm of the left superior cerebellar artery

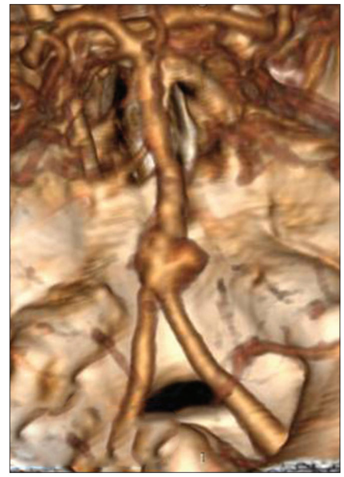

Figure 6: Volume-rendering technique image showing aneurysm at the vertebrobasilar junction

Table 3: Comparison of computed tomographic angiography and digital subtraction angiography in localization of aneurysms (percentages in parenthesis)

Location	DSA (%)	CTA (%)
Vertebral artery - V4 segment		
Right	5 (20)	6 (24)
Left	6 (24)	6 (24)
Total	11 (44)	12 (48)
PICA		
Right	3 (12)	2 (8)
Left	1 (4)	1 (4)
Total	4 (16)	3 (12)
Anterior inferior cerebellar artery		
Right	1 (4)	0
Left	2 (8)	2 (8)
Total	3 (12)	2 (8)
Superior cerebellar artery		
Right	1 (4)	1 (4)
Left	0	0
Total	1 (4)	1 (4)
Vertebrobasilar junction	1 (4)	1 (4)
Mid-BA	3 (12)	3 (12)

BA – Basilar artery; DSA – Digital subtraction angiography; CTA – CT angiography; CT – Computed tomographic; PICA – Posterior inferior cerebellar artery

Table 4: Diagnostic efficacy of computed tomographic angiography in aneurysmal size

	Sensitivity (%)	Specificity (%)	Positive predictive value (%)	Negative predictive value (%)
<4 mm	83.3	100	100	95
>4 mm	100	100	100	100

was performed in 17 (36.2%) patients, of which 41.2% were for PICA aneurysms. Stent-associated coiling was done in 7 (14.9%) patients, of which six patients had vertebral artery aneurysms and one patient had aneurysm in mid-BA. Two patients with vertebral artery aneurysms underwent coiling with parent vessel occlusion.

Discussion

The increased morbidity and mortality associated with posterior fossa bleeds and vascular pathologies necessitates their rapid and correct diagnosis. DSA has been considered as imaging gold standard in investigation of SAH. Recent advancements in CT angiography technique and it being non-invasive with no procedural neurological complications, add to the advantages with CTA.

The most common cause of nontraumatic SAH is aneurysm.[1] The most common site of aneurysm was vertebral artery, accounting for 37% of cases in the posterior fossa in our study. Among the cerebellar arteries, the most common artery was PICA (25.5%). According to the literature, the most common site of aneurysm among posterior circulation was basilar top, followed by PICA.[12] However, we included arteries of the posterior fossa and not included posterior circulation. Hence, the basilar top was not included in our study. We found vertebral artery being the most common site and dissecting aneurysms as common etiology.

A number of research studies have been performed to evaluate MDCTA in diagnosis of intracranial aneurysms, but none was specific to the posterior fossa. Initial studies which compared single-detector CT with DSA showed a sensitivity of 62%–100% and specificity of 98%–100%.[13] With advancement of MDCT, sensitivity of detecting aneurysms increased like with 16-detector CT sensitivity, specificity, and accuracy was of 95.1%, 94.1%, and 95%, respectively.[2] As number of detector increased sensitivity of detecting aneurysms increased like with 64-slice CT detector sensitivity was 95.8%[3] with 320-detector sensitivity was 96.3.[5] For aneurysms >4 mm, sensitivity of CTA is almost equal to DSA. However, for aneurysms <4 mm (<3 mm in some studies), the sensitivity

Table 5: Diagnostic efficacy of computed tomographic angiography compared to digital subtraction angiography (gold standard)

	Sensitivity (%)	Specificity (%)	Positive predictive value (%)	Negative predictive value (%)	Diagnostic accuracy (%)
Per-aneurysm basis	96	-	100	-	96
Per-patient basis for detection of aneurysms	95.7	100	100	90	96.9

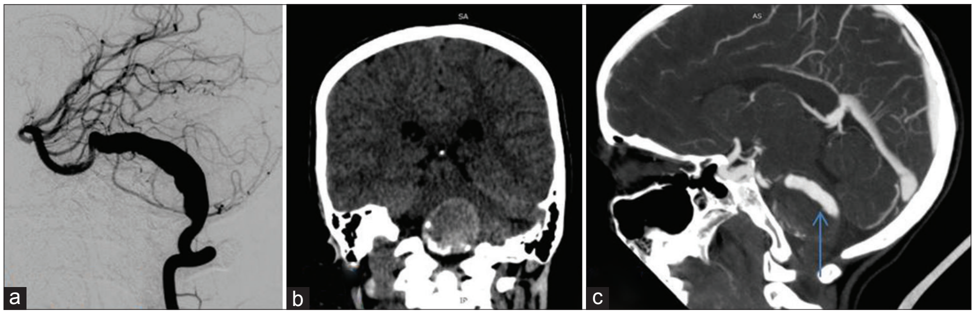

Figure 7: Thrombus detection in computed tomography angiography and digital subtraction angiography. (a) Digital subtraction angiography image in lateral view showing fusiform aneurysm involving the entire V4 segment of the right vertebral artery, (b) Noncontrast computed tomography of the same patient showing round hyperdense lesion with calcification in its inferior aspect (c) Sagittal maximum intensity projection image of the same patient showing large-rounded aneurysm of the right vertebral artery filled with thrombus and contrast visualization only in upper aspect (arrow)

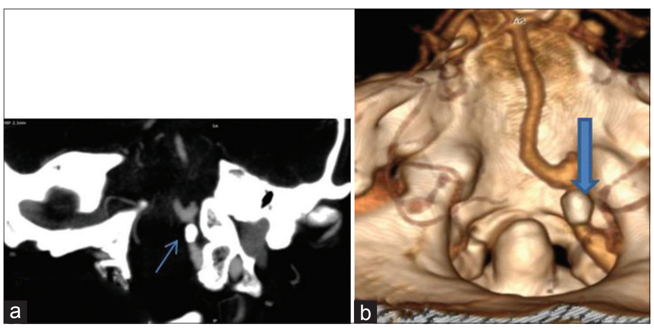

Figure 8: Calcification in aneurysm. (a) Coronal maximum intensity projection image and (b) volume-rendered image of the same patient showing calcification (thin arrow in Figure a and thick in Figure b) in the wall of aneurysm in V4 segment of the left vertebral artery

is relatively lower. According to a study by Donmez *et al*.,[2] sensitivity for detecting aneurysms <3 mm was found to be 86.1% with specificity and diagnostic accuracy of 94.1% and 88.6%, respectively. Milošević Medenica *et al*.[4] compared CTA with DSA and surgical findings and showed that sensitivity of detecting aneurysms <4 mm was only 88.8%. In our study, CTA detected 24/25 aneurysms correctly. The sensitivity of detecting aneurysms <4 mm was only 83.3% as compared to 100% sensitivity in detecting aneurysms >4 mm. The overall sensitivity in detecting the aneurysms on per-patient basis was found out to be 95.7% with diagnostic accuracy of 96.9%, which is comparable to the other studies performed. There was no statistically significant difference in sizes of aneurysms detected between CTA and DSA.

The low sensitivity of CTA in detecting smaller sized aneurysms can be attributed partially to lower spatial resolution of CT compared to DSA, other contributing factors being location adjacent to bony structures, especially in the posterior fossa, where aneurysms can be overlooked. In our study, missed aneurysm was located close to the skull base. However, on retrospective analysis, after looking DSA images, missed aneurysm could be detected in MIP and MPR CT images. The detection of aneurysms close to the skull base and bones remains a challenging issue even with higher channel detector CT scans. To circumvent this problem, various postprocessing techniques have been developed, which include subtraction algorithm CTA volume subtraction (VS)-3D CTA, which allows bone-free aneurysm visualization. Sakamoto *et al*.[14] reported that VS-3D CTA detected all 29 aneurysms of ICA in 25 patients and suggested VS-3D CTA can be used as an alternative to DSA for preoperative examination of aneurysms near the skull base. In another study by Luo *et al*.,[15] on comparing 320-row subtraction CTA with 320-row nonsubtracted CTA, they showed that 320-row subtraction CTA was more powerful than nonsubtracted CTA in detecting small aneurysms as well as aneurysms adjacent to the bone. However, Ramasundara *et al*.[16] found that there was no significant difference between the diagnostic ability of bone subtraction CTA compared with CTA. The postprocessing techniques employed in our study were volume-rendered imaging (VRI) combined with MPR for determination of the aneurysms near the skull base, and we found that the aneurysms <4 mm can be delineated by careful inspection of the VRI combined with MPR images with appropriate window and level settings.

Our results suggest that MDCTA can yield valuable information regarding the localization and the size of aneurysms. MDCTA uses a more quantitative measurement method which gives more precise results. In our study, we used MPR and MIP images mainly for measurements. VRI

Table 6: Therapeutic procedures performed in patients with aneurysms

Therapeutic procedures	*n*
Total cases	47
Treatment	27
Endovascular	26
Coiling	17
Stent-associated coiling	7
Coiling + parent vessel occlusion	2
Surgical clipping	1

was used rarely for measurement, as the measurement in VRI changes significantly with small changes in threshold settings. The other main advantage of CTA is that it can detect the presence of mural calcifications and intraluminal thrombus, as was the case in our study [Figures 7 and 8]. CTA is superior to DSA in detection of calcifications and thrombus.[17] The presence of calcification at level of the neck of aneurysm can lead to difficulty in clipping of sac during surgery, and intraluminal thrombus poses a threat of distal emboli during endovascular coiling. Hence, CTA can play an important role in deciding the treatment plan.

3D-CTA has added advantage of able to reconstruct the image in any desired plane or angle using VRI technique. Thus, the best plane which helps in visualization of aneurysmal sac and branching vessels can be found by swiveling the VRI images. Conventional DSA can provide only 2D images; hence, various projections needed to be taken in order to delineate the surrounding vascular anatomy. Similar to 3D-CTA, 3D-DSA has been introduced in recent times, which can reconstruct the image in any chosen projection. It has been shown that 3D-DSA can detect more occult aneurysms and morphology of the arteriovenous malformations as compared to the conventional 2D-DSA.

The main limitation of our study was small sample size for comparison of CTA and DSA. Some of the patients were referred to our institution from outside with the diagnosis of SAH, and CTA was not repeated in such cases due to ethical reasons. Even though our sample size was comparatively lower, the sensitivity of CTA in comparison to DSA was similar to that obtained in other studies from literature, for aneurysms. The other limitation was the unavoidable selection bias in which older patients with spontaneous intraparenchymal hemorrhage were not taken up for the study due to their health conditions.

Conclusion

CTA is a simple, fast, and noninvasive imaging modality that can be used to detect and characterize the intracranial aneurysms in the posterior fossa. The overall sensitivity in detecting the aneurysms is 96% with sensitivity in detecting aneurysms >4 mm being 100%. The diagnostic accuracy in detecting the aneurysms on per-patient basis is 96.9%. The only limitation with CTA is the lower sensitivity in detecting aneurysms <4 mm (83%). CTA is able to precisely depict the aneurysmal morphology which might help in treatment planning. CT also has some advantages compared to DSA in detecting the calcifications and intraluminal thrombus. CTA though have a drawback in posterior fossa as more of compact bony structures are there but can be used in the initial investigation for SAH and could be helpful in the diagnosis and characterization of aneurysms in the posterior fossa and their treatment planning.

Financial support and sponsorship

Nil.

Conflicts of interest

There are no conflicts of interest.

References

1. Osborn AG. Osborn's Brain – Imaging, Pathology and Anatomy. 1st ed. Philadelphia: USA Lippincott Williams and Wilkins; 2013.
2. Donmez H, Serifov E, Kahriman G, Mavili E, Durak AC, Menkü A, *et al.* Comparison of 16-row multislice CT angiography with conventional angiography for detection and evaluation of intracranial aneurysms. Eur J Radiol 2011;80:455-61.
3. Li Q, Lv F, Yao G, Li Y, Xie P. 64-section multidetector CT angiography for evaluation of intracranial aneurysms: Comparison with 3D rotational angiography. Acta Radiol 2014;55:840-6.
4. Milošević Medenica S, Vućković VV, Prstojević B. 64-slice CT angiography in the detection of intracranial aneurysms: Comparison with DSA and surgical findings. Neuroradiol J 2010;23:55-61.
5. Wang H, Li W, He H, Luo L, Chen C, Guo Y, *et al.* 320-detector row CT angiography for detection and evaluation of intracranial aneurysms: Comparison with conventional digital subtraction angiography. Clin Radiol 2013;68:e15-20.
6. Neacsu A, Ciurea AV. General considerations on posterior fossa arteriovenous malformations (clinics, imaging and therapy). Actual concepts and literature review. J Med Life 2010;3:26-35.
7. Han J, Lee HK, Cho TG, Moon JG, Kim CH. Management and outcome of spontaneous cerebellar hemorrhage. J Cerebrovasc Endovasc Neurosurg 2015;17:185-93.
8. Peker A, Peker E, Akmangit I, Erden I. Comparison of 64 dedector cranial CT angiography with intra-arterial DSA for detection of intracranial aneurysms. Eur J Gen Med 2014;11:136-40.
9. Klingebiel R, Kentenich M, Bauknecht HC, Masuhr F, Siebert E, Busch M, *et al.* Comparative evaluation of 64-slice CT angiography and digital subtraction angiography in assessing the cervicocranial vasculature. Vasc Health Risk Manag 2008;4:901-7.
10. Leffers AM, Wagner A. Neurologic complications of cerebral angiography. A retrospective study of complication rate and patient risk factors. Acta Radiol 2000;41:204-10.
11. Bendszus M, Koltzenburg M, Burger R, Warmuth-Metz M, Hofmann E, Solymosi L, *et al.* Silent embolism in diagnostic cerebral angiography and neurointerventional procedures: A prospective study. Lancet 1999;354:1594-7.
12. Menke J, Larsen J, Kallenberg K. Diagnosing cerebral aneurysms

by computed tomographic angiography: Meta-analysis. Ann Neurol 2011;69:646-54.

13. Anderson GB, Steinke DE, Petruk KC, Ashforth R, Findlay JM. Computed tomographic angiography versus digital subtraction angiography for the diagnosis and early treatment of ruptured intracranial aneurysms. Neurosurgery 1999;45:1315-20.
14. Sakamoto S, Kiura Y, Shibukawa M, Ohba S, Arita K, Kurisu K, *et al*. Subtracted 3D CT angiography for evaluation of internal carotid artery aneurysms: Comparison with conventional digital subtraction angiography. AJNR Am J Neuroradiol 2006;27:1332-7.
15. Luo Z, Wang D, Sun X, Zhang T, Liu F, Dong D, *et al*. Comparison of the accuracy of subtraction CT angiography performed on 320-detector row volume CT with conventional CT angiography for diagnosis of intracranial aneurysms. Eur J Radiol 2012;81:118-22.
16. Ramasundara S, Mitchell PJ, Dowling RJ. Bone subtraction CT angiography for the detection of intracranial aneurysms. J Med Imaging Radiat Oncol 2010;54:526-33.
17. Kokkinis C, Vlychou M, Zavras GM, Hadjigeorgiou GM, Papadimitriou A, Fezoulidis IV, *et al*. The role of 3D-computed tomography angiography (3D-CTA) in investigation of spontaneous subarachnoid haemorrhage: Comparison with digital subtraction angiography (DSA) and surgical findings. Br J Neurosurg 2008;22:71-8.